

*Full Length Research Paper***Guiding of light with pinholes****Makoto Morinaga**

Institute for Laser Science, University of Electro-Communications Chofu, Tokyo, 182-8585 Japan.

Received 30 July, 2014; Accepted 8 October, 2014

A new type of light waveguide using linearly aligned pinholes is presented. Results of basic experiments are compared with theoretical estimates calculated using continuous model. This model predicts that the loss per unit length of the light inside this waveguide is proportional to the square root of the spacing between the pinholes. Since this waveguide utilizes no transparent material, it can be used to guide electromagnetic waves of wide wavelength ranges as well as other waves such as matter waves.

Key words: Waveguide, diffraction optics, atom optics.

INTRODUCTION

Waveguides for electromagnetic fields are widely used to transmit power as well as information. Classical waveguides for electromagnetic fields ranges from coaxial cables for radio frequency (RF) fields, metal waveguides for microwave fields to dielectric waveguides (optical fibers) for optical fields (Cronin, 1995). Among them optical fibers bear extremely low transmission loss and are widely used not only for classical communication (Agrawal, 2010) but also for quantum communication (Gisin, et al., 2006). Also photonic crystals have been implemented recently (Skorobogatiy and Yang, 2009). All of them require special media of high transmissivity and/or high reflectivity. In this paper, we propose a new type of waveguide composed of linearly aligned pinholes of same diameter (Figure 1).

Such a structure is meaningless in geometrical optics since whether a ray transmits through this structure depends only on the geometrical arrangement of the ray and the first and the last pinholes, and pinholes in between play no role for the transmission. However, if we

treat light as wave, it turns out that the transmission loss

at each pinhole has a form $\beta \left(\frac{\lambda L}{a^2} \right)^{\frac{3}{2}}$ where λ is the wavelength of the light, L is the spacing between pinholes, a is the radius of the pinholes, and β is a constant that depends on the order of the transverse mode of the light (Figure 1). Thus the transmission loss per unit length is proportional to \sqrt{L} so that it can in principle be made arbitrarily small by making the spacing L between the pinholes smaller and smaller. Since no special material is required for its construction, it can be used to guide electromagnetic fields of wide frequency ranges, or waves of other kinds such as matter waves. Or it can also be used to guide and/or confine atoms with light guided by this pinhole waveguide because the space where light passes through is vacant. In the following, we present basic experiments with pinhole waveguides and, in the appendix, we will outline a theoretical treatment of this waveguide using continuous model to analyze the

* E-mail: morinaga@ils.uec.ac.jp

Author(s) agree that this article remain permanently open access under the terms of the [Creative Commons Attribution License 4.0 International License](https://creativecommons.org/licenses/by/4.0/)

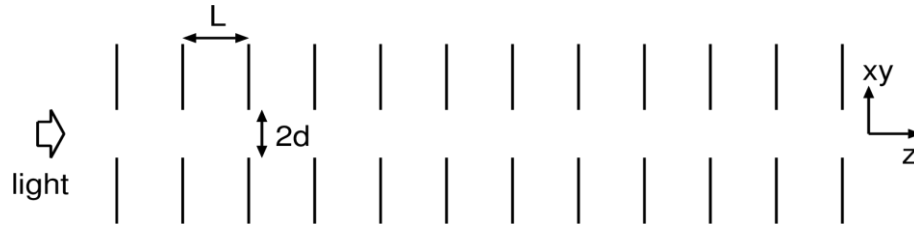


Figure 1. Construction of the pinhole waveguide. Pinholes of radius d are aligned on a straight line with spacing L between the pinholes.

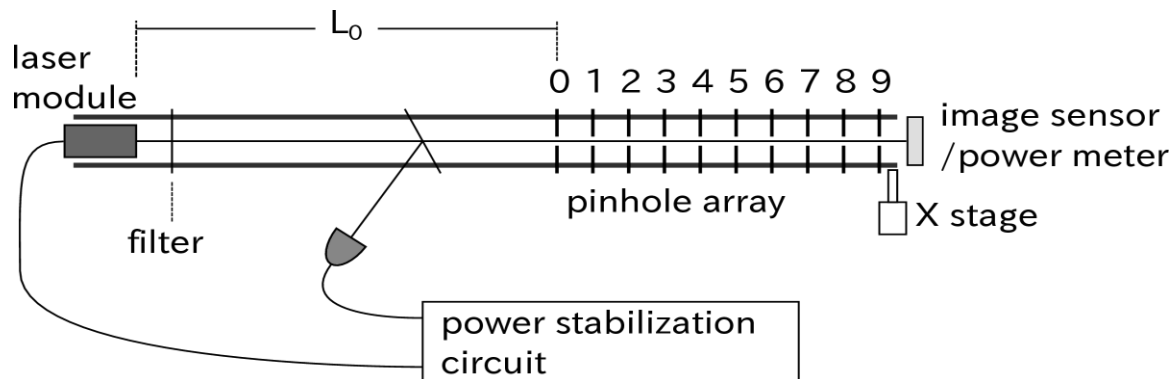


Figure 2. Light from a laser module propagates through pinholes and is detected by either an image sensor or a power meter at the end of the pinhole array which also can be inserted in between the pinholes. Filters are used to select 1064 nm/532 nm wavelengths. The distance L_0 between the laser module and the 1st pinhole is 450 mm.

experimental results. For an array of slits, see (Morinaga, 2014) for asymptotic analysis and numerical simulation that calculate the diffraction directly.

EXPERIMENTS WITH PINHOLE WAVEGUIDES

The experimental setup is schematically shown in Figure 2. A Diode Pumped Solid State (DPSS) laser module generates TEM_{00} output of wavelength at both 1064 and 532 nm. 1064 nm (532 nm) wavelength is selected by inserting a visible cut filter (infrared cut filter). Part of the laser beam is reflected into a photo diode for power stabilization. When the laser beam enters the pinhole array, the beam size is considerably larger than the size of the pinhole and we can regard the incident wave as a spherical wave. Each pinhole is mounted on a xy -translation stage which is fixed on a linear rail lying in z -direction. Up to 10 pinholes can be set on the rail with minimum spacing of 15 mm (29 mm to insert the image sensor or the power meter between the pinholes).

Pinhole alignment

The alignment procedure of the pinholes on a straight line

is as follows. The power meter is always set at the end of the pinhole array during this procedure and the light at 532 nm wavelength is used. First we set no pinhole except the last pinhole (pinhole no.9 in Figure 2) and maximize the power by adjusting the xy -position of this pinhole (the power is plotted as '0' in the horizontal axis of Figure 3). Next we set the first pinhole (pinhole no.0 in Figure 2) and maximize the power by adjusting the xy -position of this pinhole (plotted as '1' in the horizontal axis of Figure 3). And then pinhole no.1 (plotted as '2'), pinhole no.2 (plotted as '3'), and so on. The spacing between the pinholes is $L=45$ mm. The measured values are compared with simulated values obtained by calculating the sequential diffraction by the pinholes. From Figure 3, we see that the transmitted light power increases with increasing number of pinholes, which cannot be explained by geometrical optics.

Propagation through the pinhole array

After setting and aligning all the 10 pinholes light power after each pinhole is measured and compared with the theoretical curve calculated using the Equation (19) in the appendix (Figure 4). In the calculation we neglected the curvature of the wavefront of the input laser so that the

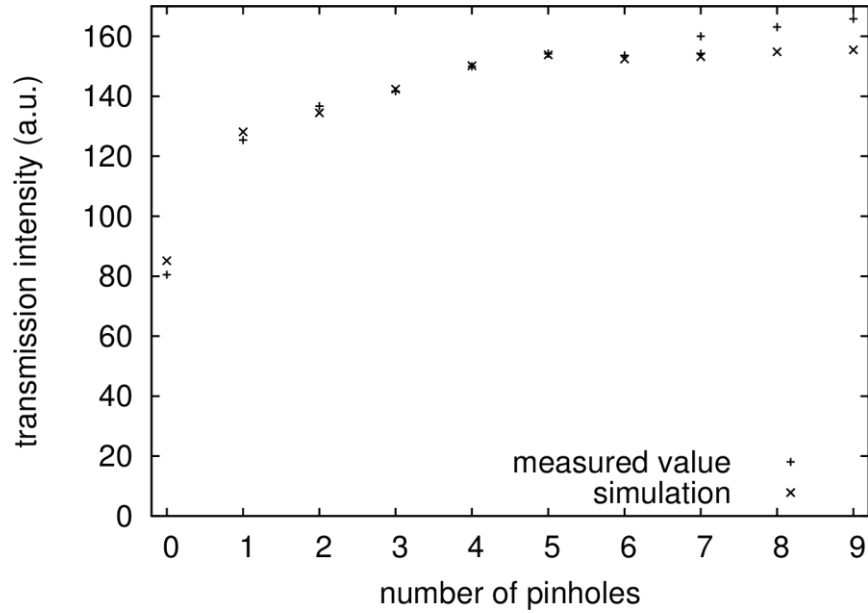


Figure 3. The power of the output of the pinhole array is plotted while inserting pinholes one by one. Pinhole diameter: $2d=0.5$ mm. Light wavelength: $\lambda=532$ nm. Calculated values are also plotted for comparison.

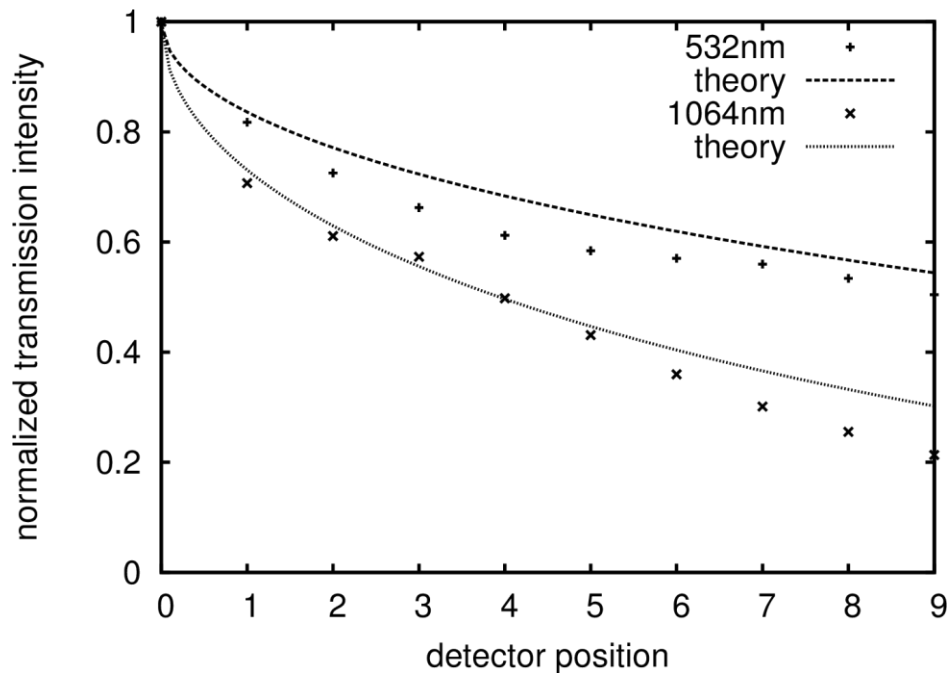


Figure 4. Light power after each pinhole is plotted. The power after the pinhole no.0 is normalized to 1. Pinhole spacing: $L=45$ mm. $2d=0.5$ mm. Two lines are theoretical curves calculated using the continuous model (Equation (19)).

incident wave is assumed to be a plane wave and we used the value of ξ given in Equation (1). The theoretical curves are plotted with no fitting parameter except that the

initial power is normalized to 1 for both experiment and theory. The tendency that the experimental value is lower than the theoretical curve might be explained by the fact

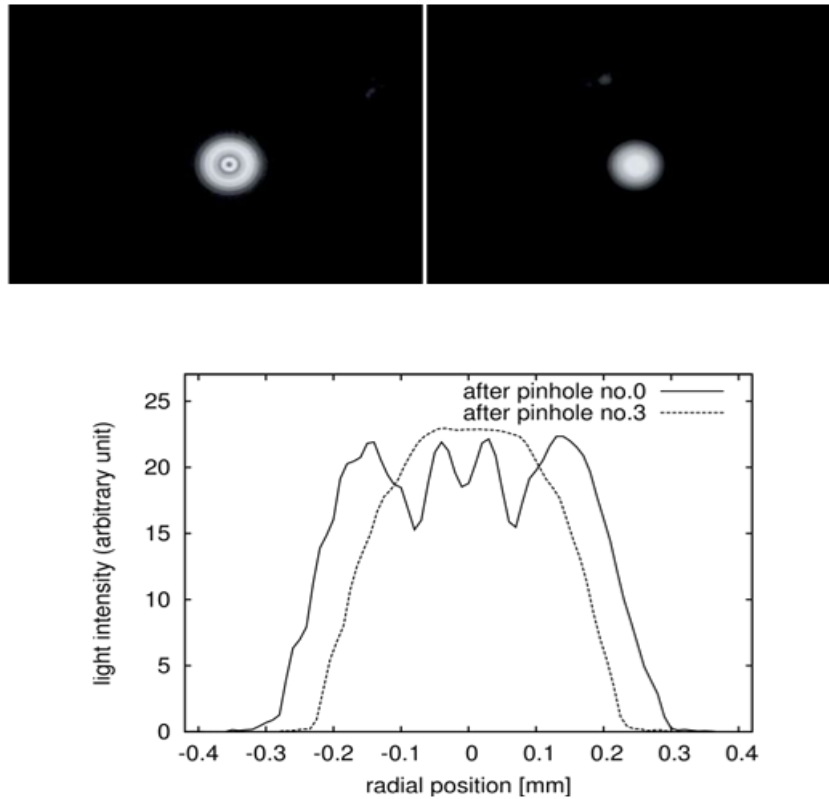


Figure 5. Beam images after pinhole no.0 (left image) and pinhole no.3 (right image). The graph shows their radial distributions.

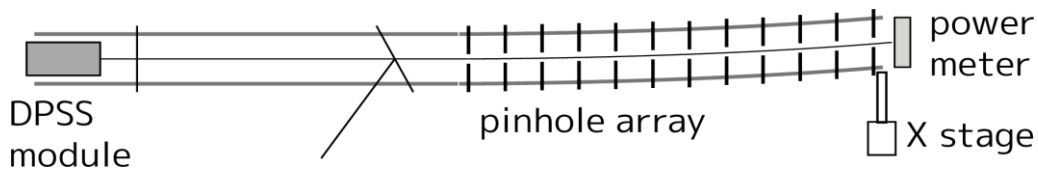


Figure 6. Schematics of the light bending experiment.

that the misalignment of the pinhole always decreases the power from that without misalignment. The initial square beam cut out from the incident plane wave contains high order transverse modes that attenuate fast compared with the lower order mode leading to the initial rapid decay. After propagating through several pinholes, lowest order mode dominates, then showing slower decay.

In Figure 5 beam images after the pinhole no.0 and no.3 are shown ($\lambda=532$ nm). The latter shows smooth profile with a peak intensity at the center which qualitatively confirms the explanation given above (the distance of about 17 mm from the pinhole to the image sensor makes fine structure in the left image due to diffraction).

Bending of light

The linear rail on which pinholes is sitting is fixed to the

optical table at three points: at the left end, in the middle near the pinhole no.0, and at the right end. We remove the fixing screw at the right end and push this end to the transverse direction so that the rail is bent elastically (Figure 6).

In Figure 7 we plot the power of the output light versus the displacement of the last pinhole (pinhole no.9). The experimental value is compared with a theoretical curve assuming the geometrical optics.

Certain amount of light is transmitted even with displacements larger than the diameter of the pinhole (0.5 mm). The measured values are also compared with a theoretical curve using a simplified model: the guided light experiences several (additional) reflections inside the waveguide when the waveguide is bent. Sum of the reflection angle Θ_j (measured from the reflection surface) is equal to a half of the bending angle Θ of the

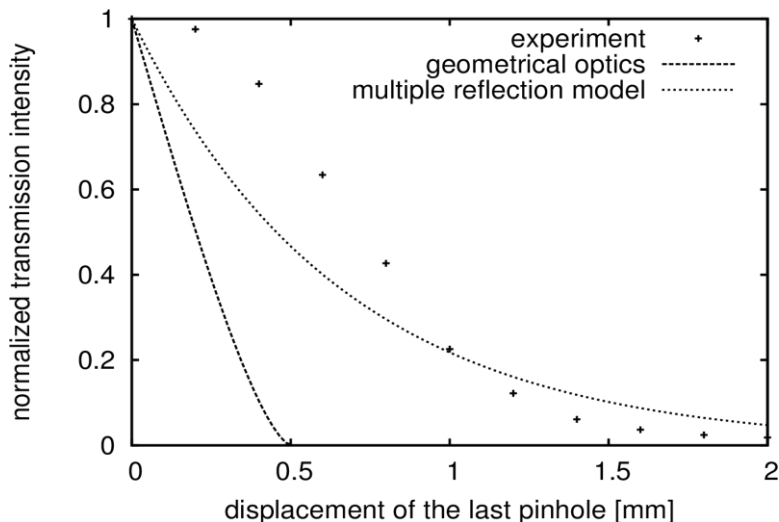


Figure 7. Power of the transmitted light is measured while bending the waveguide. $2d=0.5$ mm. $\lambda=532$ nm. $L=45$ mm. Dotted line is the theoretical curve following the geometrical optics. The measured values are also compared with a theoretical curve.

waveguide at the output end: $\sum_i \Theta_i = \Theta/2$. The power loss at each reflection is known to be $4\sqrt{\pi L/\lambda}\Theta_i$ when $\Theta_i \ll \sqrt{\lambda L}$ (Kouznetsov and Oberst, 2005b). The final output power I is calculated as $I = I_0 \prod_i \exp(-4\sqrt{\pi L/\lambda}\Theta_i) = I_0 \exp(-2\sqrt{\pi L/\lambda}\Theta) = I_0 \exp(-\sqrt{\pi L/\lambda} \frac{3\delta}{L_1})$ where I_0 is the input power, δ is the transverse displacement at the output end, and $L_1=405$ mm is the total length of the waveguide. Here we also used the relation $\Theta = \frac{3\delta}{2L_1}$ derived from the elementary mechanics.

The agreement is acceptable taking into account that no fitting parameter is used in the calculation although the discrepancy is apparent when the displacement is small. This is because the model does not include the notion of mode spacing which would prevent mixing of modes for small bending.

CONCLUSION AND OUTLOOK

In this paper we presented basic experiments of light guiding with a pinhole array. A theoretical study using a continuous model was also developed which predicts that the loss per unit length is proportional to the square root of the spacing between the pinholes. The experimental results roughly confirm the theoretical estimates. However, further study is needed to understand the details of this new waveguide, such as how the thickness of the

pinholes affects the transmission. Also a refined theory is needed to explain the transmission behavior quantitatively when the pinhole array is bent.

Conflict of Interest

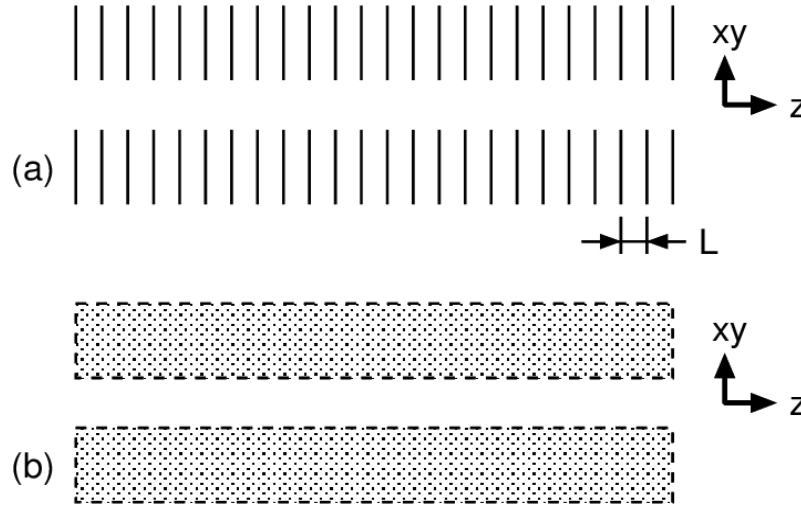
The authors have not declared any conflict of interest.

ACKNOWLEDGEMENT

This work was partly supported by the AMADA FOUNDATION and the Photon Frontier Network Program (MEXT).

REFERENCES

- Agrawal GP (2010). Fiber-Optic Communication Systems, 4th ed., John Wiley & Sons.
- Cronin N J (1995). Microwave and Optical Waveguides, CRC Press.
- Gisin N, Iblisdir S, Tittel W, Zbinden H (2006). Quantum Communications with Optical Fibers, in: A. V. Sergienko (Eds.), Quantum Communications and Cryptography, Taylor & Francis Chapter 2.
- Kouznetsov D, Morinaga M (2012). Guiding of waves between absorbing walls. J. Mod. Phys. 3 553. <http://dx.doi.org/10.4236/jmp.2012.37076>
- Kouznetsov D, Oberst H (2005a). 1. Reflection of waves from a ridged surface and the Zeno effect, Opt. Rev. 12: 363. <http://dx.doi.org/10.1007/s10043-005-0363-9>
- Kouznetsov D, Oberst H (2005b). 2. D. Kouznetsov and H. Oberst, Scattering of waves at ridged mirrors, Phys. Rev. A 72: 013617. <http://dx.doi.org/10.1103/PhysRevA.72.013617>
- Morinaga M (2014). Wave propagation through an array of slits, arXiv:1409.6865
- NIST Digital Library of Mathematical Functions §10.17. <http://dlmf.nist.gov/10.17>
- Skorobogatiy M, Yang J (2009). Fundamentals of Photonic Crystal Guiding, Cambridge University Press.



Appendix Figure 1. (a) Array of masks separated by L . (b) The mask array is replaced with continuous absorbing medium.

APPENDIX

Continuous model

Dealing directly with a discrete array of masks (pinholes, slits,...) for theoretical analysis is not an easy task. Instead, we introduce in this appendix a model in which the discrete set of masks is replaced with continuous medium of some absorbance that fills the closed region of the masks (Appendix Figure 1). This continuous model was first introduced for an array of half-planes to account the enhanced quantum reflection of matter waves from the ridged surfaces (Kouznetsov and Oberst, 2005a). The lowest order transverse mode function for the slit array and its loss parameter are also calculated already (Kouznetsov and Morinaga, 2012). Here we will determine all the transverse mode functions and their propagation parameter for the case of the slit array and the pinhole array. The light field is treated as a scalar field (scalar theory). The wave equation for this model is given by

$$-k_0^2 \psi(x, y, z) = \{1 - i\epsilon \Theta(x, y)\} \nabla^2 \psi(x, y, z)$$

where k_0 is the wavenumber of light, $\Theta(x, y)$ is a step function that takes value 1 (0) in the closed (open) region of masks, and ϵ is a positive constant related to the absorbance of the medium. As we shall see below $\epsilon \ll 1$ for our system under consideration. First we consider a plane wave propagating through the area filled uniformly with such absorbing medium. Taking z -axis as the direction of propagation, the wave equation is written as:

$$-k_0^2 \psi(z) = (1 - i\epsilon) \psi''(z).$$

Its solution is given by

$$\psi(z) = e^{ik_z z}$$

with $k_0^2 = (1 - i\epsilon) k_z^2 \approx \left\{ \left(1 + \frac{i}{2\epsilon}\right)^{-1} k_z \right\}^2$ so that $k_z = \left(1 + \frac{i}{2\epsilon}\right) k_0$ and $|\psi(z)|^2 = e^{-\zeta_0 z}$ with the intensity absorbance $\zeta_0 = \epsilon k_0$. Given that this absorbing medium imitates a stack of opaque masks separated by a distance L , we expect that $\zeta_0 \sim \frac{1}{L}$ so that $\epsilon \sim \frac{1}{k_0 L}$. Thus we shall

write $\epsilon = \frac{\xi}{k_0 L}$ with a positive parameter ξ of order of 1.

We consider the parameter region where the separation of masks L is much larger than the wavelength, so that $\epsilon \ll 1$. The continuous model itself cannot determine the value of ξ (or ϵ). By comparing the attenuation of a wave propagating in a slit waveguide calculated using continuous model with that calculated with direct method (Morinaga, 2014) it is shown that

$$\xi = \frac{9}{2\pi}. \quad (1)$$

A.1 Slit array

Consider an array of slits of opening width $2d$ (open for $|x| < d$). The wave equation is written as:

$$-k_0^2 \psi(x, z) = \{1 - i\epsilon \Theta(x^2 - d^2)\} (\partial_x^2 + \partial_z^2) \psi(x, z)$$

where Θ is the conventional step function defined as:

$$\Theta(s) \equiv \begin{cases} 0 (s < 0) \\ 1 (s \geq 0) \end{cases}$$

Because of the translational symmetry in z-axis direction, we can assume the form of the solution as $\psi(x,z) = \phi(x) e^{ik_z z}$ (a general solution is the sum of such solutions). Below we also assume that the wave propagates nearly in z direction so that $k_z \approx k_0$.

Region A (inside the opening of slits) $|x| \leq d$

The wave equation for the transverse wavefunction $\phi(x)$ here is

$$-(k_0^2 - k_z^2)\phi(x) = \phi''(x)$$

with a solution

$$\phi(x) = cs(k_A x),$$

where cs is defined as

$$cs(u) = \begin{cases} \cos u & (\text{even parity mode}) \\ \sin u & (\text{odd parity mode}) \end{cases} \quad (2)$$

and k_A satisfies $k_0^2 = k_A^2 + k_z^2$. We are considering the situation in which the wave is nearly confined in the opening region $|x| \leq d$ and hence $\phi(\pm d) \approx 0$, so that

$$k_A d \approx \frac{n+1}{2} \pi \quad (n=0, 1, 2, \dots)$$

provided that we use \cos (\sin) in (2) for even (odd) n . Defining $k_n \equiv \frac{n+1}{2d} \pi$ and write $k_A = k_n + \beta + i\gamma$ with real numbers β and γ , then $|\beta d| \ll 1$ and $|\gamma d| \ll 1$.

$$\phi(\pm d) = cs(\pm k_A d) \approx \pm (\beta + i\gamma) d cs'(\pm k_n d)$$

$$\phi'(\pm d) = k_A cs'(\pm k_A d) \approx k_n cs'(\pm k_n d)$$

$$\left. \frac{\phi'}{\phi} \right|_{x=\pm d} \approx \pm \frac{k_n}{(\beta + i\gamma)d} \quad (3)$$

Region B (outside the opening of slits): $|x| \geq d$

Here the wave equation is

$$-\{k_0^2 - (1-i\epsilon)k_z^2\}\phi(x) = (1-i\epsilon)\phi''(x)$$

so that the solution is, taking into account that it should not diverge when $x \rightarrow \pm\infty$,

$$\phi(x) \propto e^{ik_B |x|} \quad (4)$$

where k_B satisfies $k_0^2 = (1-i\epsilon)(k_B^2 + k_z^2)$ and $\text{Im } k_B > 0$ (the proportionality factor in Equation (4) has opposite sign for $x \geq d$ and $x \leq -d$ for the odd parity solution). Thus

$$\left. \frac{\phi'}{\phi} \right|_{x=\pm d} = \pm ik_B \quad (5)$$

Boundary condition at $x = \pm d$

By requiring $\phi(x)$ and $\phi'(x)$ is continuous at $x = \pm d$, from Equations (3) and (5) we find

$$ik_B = \frac{k_n}{(\beta + i\gamma)d} \quad (6)$$

By noting $k_B^2 - k_A^2 = \frac{i\epsilon}{1-i\epsilon} k_0^2$ and $|k_B| = \frac{|k_n|}{|\beta + i\gamma|d} \gg |k_n| \approx |k_A|$, we see

$$k_B^2 \approx i\epsilon k_0^2 \quad (7)$$

so that

$$k_B = \frac{1+i}{\sqrt{2}} \sqrt{\epsilon} k_0 \quad (8)$$

Using Equation (6)

$$\beta + i\gamma = \frac{k_n}{ik_B d} = \frac{1+i}{\sqrt{2}} \frac{k_n}{\sqrt{\epsilon} k_0 d}$$

and we obtain

$$k_A = k_n + \beta + i\gamma = \left(1 - \frac{1+i}{\sqrt{2\epsilon} k_0 d}\right) k_n \quad (9)$$

From the assumption that $|\beta d| \ll 1$ and $|\gamma d| \ll 1$ we see $\sqrt{\epsilon} k_0 d \gg 1$, that is,

$$\frac{L}{k_0 d^2} = \frac{1}{2\pi} \frac{\lambda L}{d^2} \ll 1. \quad (10)$$

Finally k_z is derived as

$$k_z = \sqrt{k_0^2 - k_A^2} \approx k_0 - \frac{1}{2} \frac{k_A^2}{k_0} \approx k_0 - \frac{k_n^2}{2k_0} + \frac{k_n^2}{\sqrt{2\varepsilon} k_0^2 d} \quad (11)$$

From this we calculate the light attenuation along the waveguide

$$|e^{ik_z z}|^2 = e^{-\zeta z}$$

where the attenuation coefficient $\zeta = 2\text{Im} k_z$ is calculated as

$$\zeta = \frac{\sqrt{2} k_n^2}{\sqrt{\varepsilon} k_0^2 d} = (n+1)^2 \frac{\sqrt{2} \pi^2}{4 \sqrt{\varepsilon} k_0^2 d^3} = (n+1)^2 \frac{\sqrt{2L} \pi^2}{4 \sqrt{\varepsilon} k_0^3 d^3}$$

using $\varepsilon = \frac{\xi}{k_0 L}$. The attenuation per length L (that is, per one slit) ζL can be written as a function of a single dimensionless parameter $\frac{\lambda L}{d^2}$:

$$\zeta L = (n+1)^2 \frac{\sqrt{2} \pi^2}{4 \sqrt{\xi}} \left(\frac{L}{k_0 d^2} \right)^{\frac{3}{2}} = (n+1)^2 \frac{\sqrt{\pi}}{8 \sqrt{\xi}} \left(\frac{\lambda L}{d^2} \right)^{\frac{3}{2}} \quad (12)$$

A.2 Pinhole array

In the case of an array of pinholes of diameter d , using cylindrical coordinate (r, φ, z) , the wave equation is written as

$$-k_0^2 \psi(r, \varphi, z) = \{1 - i\varepsilon \Theta(r^2 - d^2)\} \left(\partial_r^2 + \frac{1}{r} \partial_r + \frac{1}{r^2} \partial_\varphi^2 + \partial_z^2 \right) \psi(r, \varphi, z).$$

In the same way as in the case of slit array, we shall derive a solution of the form $\psi(r, \varphi, z) = \phi(r, \varphi) e^{ik_z z}$ with $k_z \approx k_0$.

Region A (inside the opening of pinholes): $|r| \leq d$

The wave equation

$$-(k_0^2 - k_z^2) \phi(r, \varphi) = \left(\partial_r^2 + \frac{1}{r} \partial_r + \frac{1}{r^2} \partial_\varphi^2 \right) \phi(r, \varphi)$$

is solved using the Bessel functions of the 1st kind J_m ($m=0, \pm 1, \pm 2, \dots$):

$$\phi(r, \varphi) = J_m(k_A r) e^{im\varphi}$$

where k_A satisfies $k_0^2 = k_A^2 + k_z^2$. Again we postulate

$k_A d \approx \varrho_n^{(m)}$ ($n=0, 1, 2, \dots$). Here $\varrho_0^{(m)}, \varrho_1^{(m)}, \varrho_2^{(m)}, \dots$ are positive zeros of $J_m(\varrho)$ sorted in

ascending order. We define $k_n^{(m)} \equiv \frac{\varrho_n^{(m)}}{d}$ and write

$k_A = k_n^{(m)} + \beta + i\gamma$ using real numbers β and γ with $|\beta d| \ll 1$ and $|\gamma d| \ll 1$.

$$\phi(d, \varphi) = J_m(k_A d) e^{im\varphi} \approx (\beta + i\gamma) d J_m'(k_n d) e^{im\varphi}$$

$$\partial_r \phi|_{(d, \varphi)} = k_A J_m'(k_A d) e^{im\varphi} \approx k_n^{(m)} J_m'(k_n^{(m)} d) e^{im\varphi}$$

$$\left. \frac{\partial_r \phi}{\phi} \right|_{(d, \varphi)} \approx \frac{k_n^{(m)}}{(\beta + i\gamma) d} \quad (13)$$

Region B (outside the opening of pinholes): $|r| \geq d$

The wave equation is written as:

$$-\{k_0^2 - (1 - i\varepsilon) k_z^2\} \phi(r, \varphi) = (1 - i\varepsilon) \left(\partial_r^2 + \frac{1}{r} \partial_r + \frac{1}{r^2} \partial_\varphi^2 \right) \phi(r, \varphi)$$

so that the solution is given by

$$\phi \propto H_m^{(1)}(k_B r) e^{im\varphi}$$

if we take into account its behavior when $r \rightarrow \infty$ ($H_m^{(1)}$ are the Hankel functions of the 1st kind). Here k_B satisfies $k_0^2 = (1 - i\varepsilon)(k_B^2 + k_z^2)$. Noting that $k_B^2 d^2 - k_A^2 d^2 = \frac{i\varepsilon}{1 - i\varepsilon} k_0^2 d^2$ and that the absolute value of the right-hand side is much larger than 1 (Equation (10)) whereas $k_A d$ in the left-hand side is of order of 1 so that we can neglect this term and Equations (7) and (8) holds as in the case of slit array.

From these we see that $|k_B d| \gg 1$ and $\arg(k_B d) \approx \frac{\pi}{4}$ (and thus $-\pi < \arg(k_B d) < 2\pi$), so that we can use the following

asymptotic form of $H_n^{(1)}$ for $\varrho = k_B d$ (see (NIST)):

$$H_m^{(1)}(\varrho) \approx \sqrt{\frac{2}{\pi \varrho}} \exp\left(i \left[\varrho - \frac{2m+1}{4} \pi \right]\right)$$

$$H_m^{(1)'}(\varrho) \approx i \sqrt{\frac{2}{\pi \varrho}} \exp\left(i \left[\varrho - \frac{2m+1}{4} \pi \right]\right)$$

Which lead to

$$\left. \frac{\partial_r \phi}{\phi} \right|_{(d, \varphi)} = ik_B \quad (14)$$

Boundary condition at $r=d$

Continuity of $\phi(r, \varphi)$ and $\partial_r \phi(r, \varphi)$ at $r=d$ yields, from Equations (13) and (14),

$$ik_B = \frac{k_n^{(m)}}{(\beta + i\gamma)d} \quad (15)$$

Equation (15) has the same form as Equation (5) with k_n replaced by $k_n^{(m)}$, so that similar to the case of slit array, we obtain

$$k_A = k_n^{(m)} + \beta + i\gamma = \left(1 - \frac{1+i}{\sqrt{2\epsilon}k_0 d}\right) k_n^{(m)}$$

$$k_z = \sqrt{k_0^2 - k_A^2} \approx k_0 - \frac{k_n^{(m)2}}{2k_0} + \frac{k_n^{(m)2}}{\sqrt{2\epsilon}k_0 d} i$$

From this the attenuation of light along the waveguide

$$|e^{ik_z z}|^2 = e^{-\zeta z}$$

is calculated giving the attenuation coefficient $\zeta = 2\text{Im} k_z$ as

$$\zeta = \frac{\sqrt{2}k_n^{(m)2}}{\sqrt{\epsilon}k_0^2 d} = \frac{\sqrt{2}\varrho_n^{(m)2}}{\sqrt{\epsilon}k_0^2 d^3} = \frac{\sqrt{2}L\varrho_n^{(m)2}}{\sqrt{\epsilon}k_0^3 d^3} \quad (16)$$

and the attenuation per length L (that is, per one pinhole) ζL is given by

$$\zeta L = \frac{\sqrt{2}\varrho_n^{(m)2}}{\sqrt{\epsilon}} \left(\frac{L}{k_0 d^2}\right)^{\frac{3}{2}} = \frac{\varrho_n^{(m)2}}{2\sqrt{\epsilon}\pi^3} \left(\frac{\lambda L}{d^2}\right)^{\frac{3}{2}} \quad (17)$$

Note that the modes with the same transverse wavenumber k_{\perp} ($k_{\perp} = k_n = \frac{n+1}{2d}\pi$ in Equation (12) for

the slits and $k_{\perp} = k_n^{(m)} = \frac{\varrho_n^{(m)2}}{d}$ in Equation (17) for the pinholes) have the same decay parameter.

A.3 Attenuation of a multi-transverse-mode light

In the previous section we estimated the attenuation of a single transverse mode wave. Each transverse mode is specified by a pair (m, n) of an integer m and a non-negative integer n , and if the wave is confined tightly enough in the pinhole waveguide, the transverse mode functions are given by

$$\phi_{mn}(r, \varphi) = \begin{cases} \alpha_{mn} J_m(k_n^{(m)} r) e^{im\varphi} & (r \leq d) \\ 0 & (r > d) \end{cases}$$

(α_{mn} are the normalization factors). Note that these are the Bessel beam transverse mode functions clipped at one of their nodes in the radial direction. The orthonormal condition is written as

$$\delta_{mm'} \delta_{nn'} = \langle \phi_{mn}, \phi_{m'n'} \rangle = \int_0^{\infty} r dr \int_0^{2\pi} d\varphi \phi_{mn}^*(r, \varphi) \phi_{m'n'}(r, \varphi).$$

Here, we consider, as an example, the case where a plane wave $\psi_p = \frac{1}{\sqrt{\pi d^2}} e^{ik_0 z}$ is incident into the

waveguide, and calculate how the wave attenuates while it propagates along the waveguide. The incident wavefront is cut out at the input end of the waveguide (we take the input end as $z=0$) giving the transverse wave function as

$$\phi_p(r, \varphi) = \frac{1}{\sqrt{\pi d^2}} \Theta(d^2 - r^2)$$

and such wavefront is, from the symmetry consideration, expanded with only $m=0$ modes:

$$\phi_p = \sum_{n=0}^{\infty} \beta_n \phi_{0n} \quad (18)$$

By integrating the square of absolute value of both sides of the above equation in (r, φ) plane, we see that $\sum_{n=0}^{\infty} |\beta_n|^2 = 1$. The power attenuation is given by

$$P(z) = \sum_{n=0}^{\infty} |\beta_n|^2 \exp(-\zeta_n^{(0)} z). \quad (19)$$

Here $\zeta_n^{(m)}$ is ζ given in Equation (16). By taking inner product of both sides of Equation (18) with ϕ_{0n} ,

$$\beta_n = \langle \varphi_{0n}, \varphi_p \rangle = 2\pi\alpha_{0n}^* \frac{1}{\sqrt{\pi d^2}} \int_0^d r dr J_0(k_n^{(0)} r) = \frac{2\sqrt{\pi}\alpha_{0n}^*}{k_n^{(0)}} J_1(\varrho_n^{(0)}) = \frac{2}{\varrho_n^{(0)}}$$

Here we used $\frac{d}{d\varrho}(\varrho J_1(\varrho)) = \varrho J_0(\varrho)$ and the value of α_{0n} derived in the next subsection (20).

A.4 Normalization factors α_{0n}

From the normalization conditions of ϕ_{0n} we find

$$1 = \langle \phi_{0n}, \phi_{0n} \rangle = 2\pi|\alpha_{0n}|^2 \int_0^d r dr J_0^2(k_n^{(0)} r) = \pi|\alpha_{0n}|^2 d^2 J_1^2(\varrho_n^{(0)}).$$

Here we used the formula

$$\frac{d}{d\varrho} \left\{ \varrho^2 \frac{J_0(\varrho)^2 + J_1(\varrho)^2}{2} \right\} = 2\varrho J_0(\varrho)^2$$

and $J_0(\varrho_n^{(0)}) = 0$. α_{0n} are determined as, besides the phase factor,

$$\alpha_{0n} = \frac{1}{\sqrt{\pi d} J_1(\varrho_n^{(0)})}. \quad (20)$$